Archives of Biochemistry and Biophysics
Vol. 395, No. 1, November 1, pp. 41–48, 2001
doi:10.1006/abbi.2001.2543, available online at http://www.idealibrary.com on IDEAL®

# Tissue Shear Deformation Stimulates Proteoglycan and Protein Biosynthesis in Bovine Cartilage Explants

Moonsoo Jin,*[,1] Eliot H. Frank,* Thomas M. Quinn,† Ernst B. Hunziker,‡ and Alan J. Grodzinsky*
**Continuum Electromechanics Group, Center for Biomedical Engineering, Department of Electrical Engineering and Computer Science, Department of Mechanical Engineering, Massachusetts Institute of Technology, Cambridge, Massachusetts; †Ecole Polytechnique Federale de Lausanne, Lausanne, Switzerland; and ‡M. E. Mueller Institute for Biomechanics, University of Bern, Switzerland, Bern, Switzerland*

Received March 27, 2001, and in revised form August 2, 2001; published online October 8, 2001

**Chondrocytes are known to sense and respond to mechanical and physicochemical stimuli by multiple regulatory pathways, including upstream signaling, transcription, translation, posttranslational modifications, and vesicular transport. Due to the complexity of identifying the biophysical phenomena that occur during cartilage loading *in vivo*, the regulatory mechanisms that govern chondrocyte mechanotransduction are not fully understood. Recent studies have shown that fluid flow during dynamic compression of cartilage explants can stimulate proteoglycan and protein synthesis. In this study, we examined the effect of deformations of cell and extracellular matrix on chondrocyte biosynthesis. We used tissue shear loading, since tissue shear causes little volumetric deformation and can thereby decouple fluid flow from cell and matrix deformation. Shear loading was applied over a wide range of frequencies, 0.01–1.0 Hz, using 1–3% sinusoidal shear strain amplitudes, and the resulting proteoglycan and protein syntheses were measured using radiolabel incorporation. In addition, quantitative autoradiography was used to investigate spatial variations in matrix biosynthesis and to correlate these variations with the spatial profiles of biophysical stimuli. Our data show that tissue shear loading at 1–3% strain amplitude stimulated the synthesis of protein by ~50% and proteoglycans by ~25% at frequencies between 0.01 and 1.0 Hz. The relatively uniform patterns of biosynthesis in the radial and vertical directions within cylindrical explants revealed by autoradiography suggest that the stimulatory effect was associated with the relatively uniform deformation caused by simple shear loading. These results suggest that chondrocytes can respond to tissue shear stress-initiated pathways for the production of collagen and proteoglycan, which include deformation of cells and pericellular matrix, even in the absence of macroscopic tissue-level fluid flow.** 

***Key Words:*** **tissue shear; collagen; proteoglycan; cartilage; chondrocytes; mechanotransduction.**

The development and maintenance of cartilage *in vivo* are regulated in part by mechanical loading, including compressive and shear deformations, and concomitant mechanical and physicochemical forces and flows (1). Soluble factors, including vitamins, hormones, growth factors, and cytokines, are known to be important regulators of chondrocyte biosynthesis and differentiation (2, 3). Therefore, investigators have studied the regulation of cartilage metabolism *in vitro* by utilizing mechanical or physicochemical stimuli and soluble factors (4–10): cyclic hydrostatic pressure, fluid-induced shear, dynamic tissue deformation, osmolarity and pH change, and growth factors. However, the mechanisms by which chondrocytes detect and respond to mechanical signals are not well understood. Such signaling mechanisms may include stretch-activated ion channels (11) and integrin–cytoskeleton machinery (12) which can trigger kinase cascades leading to changes in transcriptional regulation. Mechanical stresses may also affect chondrocyte biosynthesis at the level of translation and posttranslational modification by changing the structure of organelles such as endoplasmic reticulum and Golgi apparatus (1).

Dynamic compression of cartilage explants causes cell and matrix deformation as well as fluid flow within

[1] To whom correspondence and reprint requests should be addressed at MIT, Room 38-377, Cambridge, MA 02139. Fax: (617) 258-5239. E-mail: msjin@mit.edu.

0003-9861/01 $35.00

the extracellular matrix (ECM)[2] in the environment of the cells, mimicking these aspects of loading *in vivo*. Previous studies suggested that the increase in proteoglycan and protein synthesis caused by dynamic compression *in vitro* was associated with intratissue fluid flow, streaming potential, and cell deformation (13, 14). These studies modeled the spatial profiles of biophysical phenomena within compressed explants, including fluid flow and hydrostatic pressure, and compared them to the measured spatial profiles of newly synthesized proteoglycans using quantitative autoradiography. Tissue-level autoradiography has been extended to cell length scale with 1 $\mu$m resolution (15). These results demonstrated the importance of interstitial fluid flow to the stimulatory response of chondrocytes. Possible effects of fluid flow on cartilage metabolism include increased availability of nutrients and growth factors due to the convective transport, streaming potentials, and flow-induced shear stress. It has been speculated that each of these possible mechanisms can regulate chondrocyte biosynthesis. Also, the inhomogeneous deformation of ECM during unconfined compression of cartilage can cause differential stimulation along radial directions. However, it is not clear which stimulatory signals are the major factors responsible for the observed changes in biosynthesis.

In this study, we applied macroscopic shear deformation to cartilage explants, motivated by the notion that shear deformation of a homogeneous, isotropic poroelastic tissue will cause minimal volumetric changes and therefore minimal intratissue fluid flow or pressure gradients. We hypothesized that cell–matrix deformation induced by applied shear would stimulate chondrocyte biosynthesis even in the absence of significant fluid flow and pressure gradients. We further hypothesized that this stimulation would not vary dramatically with position in the explant if the applied shear deformation was reasonably uniform. Since the known stimulatory responses of chondrocytes to dynamic compression and hydrostatic pressure depended on the magnitudes and frequencies of the stimulus (13, 16, 17), shear loading in this study was applied at frequencies of 0.01–1.0 Hz and in the 1–3% range of shear strain, which is within the range of physiological tissue loading (1, 18). In addition to the radiolabel measurement of total protein and proteoglycan synthesis, we analyzed the spatial distribution of newly synthesized molecules using quantitative autoradiography.

[2] Abbreviations used: ECM, extracellular matrix; THD, total harmonic distortion; PBS, phosphate-buffered saline; FBS, fetal bovine serum.

## MATERIALS AND METHODS

*Isolation and culture of cartilage disks.* Cartilage disks (3 mm in diameter by 1–1.1 mm thick) were obtained from the femoropatellar groove of 1- to 2-week-old calves and maintained in Dulbecco's modified essential medium supplemented with 10 mM Hepes, 10% fetal bovine serum (FBS), 0.1 mM nonessential amino acids, additional 0.4 mM proline, 20 $\mu$g/ml ascorbate, 100 U/ml penicillin, and 100 $\mu$g/ml streptomycin.

*Application of shear deformation.* After 2–3 days in culture, anatomically matched disks were distributed to dynamic shear and static control groups. Shear and static control explants were held at 1-mm thickness in polysulfone chambers (with 0 to 10% compressive offset strain) without any adhesive material. The shear chamber was then mounted in a new incubator-housed loading instrument (see Frank *et al.* (19) for details). Dynamic shear deformation was applied to four to eight explants simultaneously by rotating the bottom half of the chamber with respect to the top half (Fig. 1A). Three separate series of experiments involving three different animals were performed using 3% dynamic shear strain amplitude at frequencies between 0.01 and 1.0 Hz (total $n$ = 13, 21, and 14 at 0.01, 0.1, and 1.0 Hz, respectively). In a separate series of experiment, 1% shear strain amplitude at 0.1 Hz was applied to a group of explants for 24 h with control explants (three experiments from three animals, total $n$ = 18). During the entire loading period, disks were incubated with 10 $\mu$Ci/ml [$^{35}$S]sulfate and 20 $\mu$Ci/ml [$^{3}$H]proline in order to assess proteoglycan and total protein synthesis, respectively. During shear deformation, the waveforms of both the applied deformation and the resulting torque were recorded every half hour (Fig. 1B). Total harmonic distortion (THD, defined as the ratio of the square root of the summed squares of the higher order harmonic amplitudes to the amplitude of the fundamental) was analyzed for all shear stress waveforms to monitor the quality of shear loading on cartilage explants.

*Biochemical analysis.* After radiolabeling, samples were washed three times over 1 h in phosphate-buffered saline (PBS) supplemented with 0.8 mM sodium sulfate and 0.5 mM L-proline at 4°C to remove unincorporated labels. All samples were solubilized in 1.0 ml protease K (100 $\mu$g/ml in 50 mM Tris–HCl and 1 mM $CaCl_2$, pH 8.0) for 12–18 h at 60°C. Aliquots of 100 $\mu$l of the protease K digests were mixed with 2 ml of scintillation fluid for counting (RackBeta 1211 counter, Pharmacia LKB Nuclear, Turku, Finland) and the counts were corrected for spillover. For DNA measurement, 100-$\mu$l digests were mixed with 2 ml of the Hoechst 33258 dye in an acrylic cuvette and the fluorescence was measured using a spectrofluorometer (SPF 500C, SLM Instruments, Urbana, IL) (20).

*Core vs ring comparison.* In a separate series of experiments (using two animals, total $n$ = 11), cartilage disks were subjected to 1% shear strain at 0.1 Hz for 24 h; matched control disks were held at the same static offset compression as before. After loading with radiolabeled media, a 2-mm-diameter core was removed from the center region of each test and control disks using a 2-mm punch, leaving an outer annular ring of tissue, using the method of Kim *et al.* (13). Radiolabel incorporation and DNA content were assessed separately for the core and ring region of each disk.

*Quantitative autoradiography.* In one experiment, matched cartilage disks were distributed to four different groups ($n$ = 6 each): a dynamic shear and control group radiolabeled with 10 $\mu$Ci/ml [$^{35}$S]sulfate and another dynamic shear and control group labeled with 20 $\mu$Ci/ml [$^{3}$H]proline. Both shear groups were subjected to dynamic shear loading at 3% strain and 0.1 Hz for 24 h. After loading in the presence of label, unincorporated label was removed by washing the explants three times over 1 h in PBS. Each disk was then cut in half at random orientation along the center axis of the cylindrical disk: one half was analyzed for radiolabel incorporation and the other half was prepared for autoradiography. Using the methods of Buschmann *et al.* (21), specimens for autoradiography were first

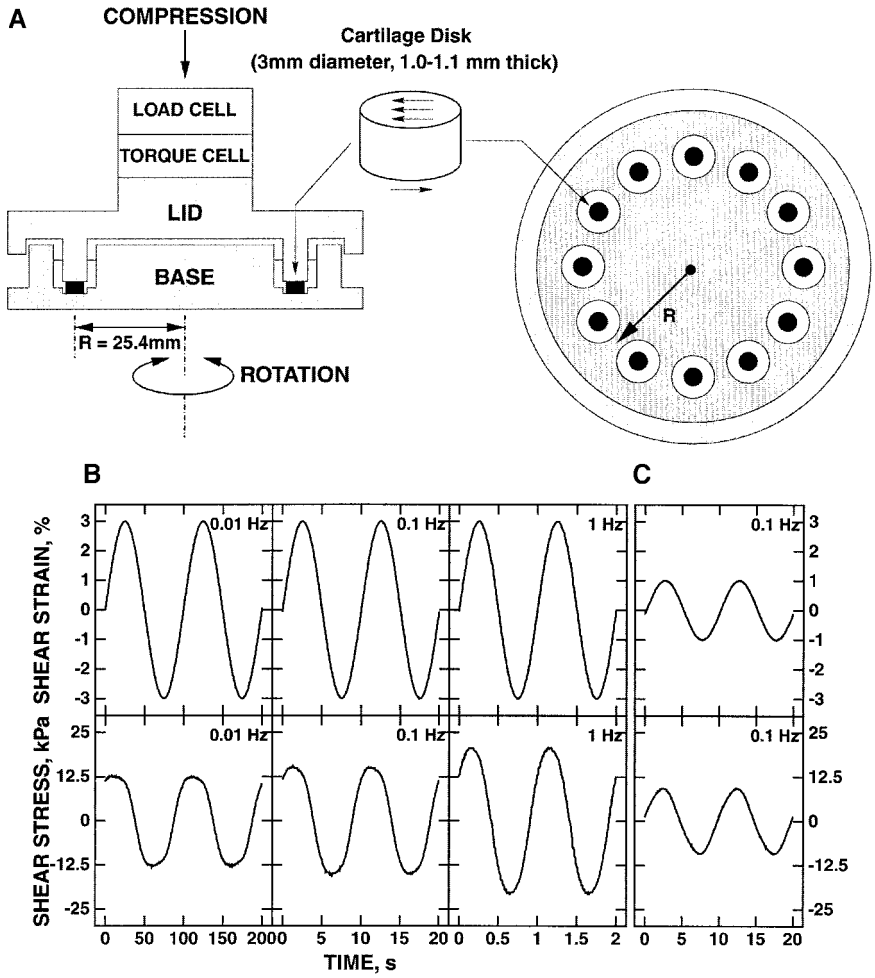


**FIG. 1.** (A) Cartilage explants were held at 1-mm thickness in the shear chamber (shown above) and static control chamber (19). The shear chamber was then mounted into the incubator-housed loading instrument, and shear strain was applied by rotating the base with respect to the top. (B) Applied shear strain at 3% amplitude; (C) shear strain at 1% amplitude. Strain waveforms were recorded from the displacement transducer, and the resulting shear stress waveforms were recorded from the torque cell throughout all experiments. The total harmonic distortions (THD) of the waveforms at 3% strain are THD = 15% at 0.01 Hz, 10% at 0.1 Hz, 3% at 1.0 Hz; and THD = 5% at 1% strain and 0.1 Hz. All strain waveforms have THD $\leq$ 0.5%.

chemically fixed in a 0.05 M sodium cacodylate buffer with 2% v/v glutaraldehyde and 2.5% w/v cetylpyridinum chloride and then dehydrated in a graded series of ethanol concentrations. Disk halves were then embedded in Epon 812, and semi-thin (1 $\mu$m) sections were obtained using an ultramicrotome. A total of 24 tissue sections were dipped in an autoradiography emulsion (Kodak NTB-2) and exposed for 2 weeks or 8 days for proline- or sulfate-labeled groups, respectively. After developing, autoradiographic images of 100 $\mu$m $\times$ 75 $\mu$m windows were captured using a high-power microscope (100$\times$ oil immersion objective, Olympus Vanox) and a CCD camera (Sony). Grain densities of each image were analyzed using IPLab software (IPLab Spectrum, Signal Analytics, Vienna, VA) with a previously developed algorithm for the tissue-length scale grain analysis (21).

*Tissue-length scale analysis of grain densities.* The grain densities of tissue sections for the 4 different dynamic shear and control groups were independently analyzed. The entire area of each 1-$\mu$m-thick disk cross section (3 mm wide $\times$ 1 mm high) obtained from all 24 disks was divided into 80 subsections corresponding to the 8 rows and 10 columns in Fig. 2A. The 80 images from these subsections were analyzed for proline or sulfate grain density. Due to the symmetry of the shear loading, the 80 images were then combined into 20 averaged subsections, representing one quadrant (1.5 mm wide $\times$ 0.5 mm high) of the cross section (Fig. 2B). Therefore, the proline and sulfate grain densities of each of the 20 subsections were obtained by averaging the grain densities of the corresponding 4 subsections grouped from 80 subsections. Variations along the radial and vertical directions were defined by grouping the corresponding sites as in Fig. 2C and 2D; the regions of center, middle, and edge were also defined along radial directions (Fig. 2E).

*Statistical analysis.* Data were represented as means $\pm$ SE. Significance of the effect of shear deformation compared to static control with no shear was identified using a two-tailed paired Student's *t* test with unequal variances. Trends of grain densities along the radial and vertical directions were identified by one-way analysis of variance (ANOVA). A power analysis was performed for the comparison of radiolabel incorporation between core and ring region in addition to the *t* test. The expression, 1-*power*, gives the frequency of making a type II error, which is accepting a false null hypothesis (a power of $>$90% is considered reliable for accepting the null hypothesis (23)). Statistical analysis of the radial and vertical variations of

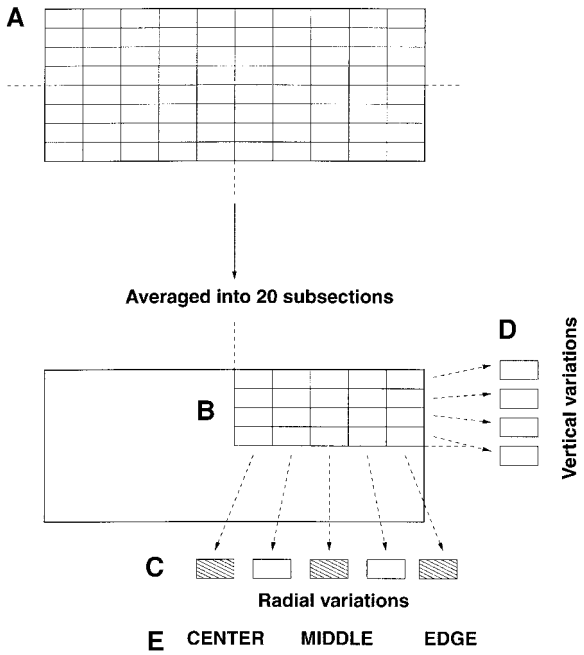


**FIG. 2.** (A) The cross section of each cartilage disk (3 mm wide × 1 mm high × 1 $\mu$m thick) was subdivided into 80 subsections (10 radial by 8 vertical). (B) Due to the symmetry of shear deformation, these 80 subsections were combined into 20 averaged subsections, representing one quadrant (1.5 mm wide × 0.5 mm high) of the cross section. (C and D) To calculate grain density variations in the radial and vertical directions, the 20 averaged subsections of (B) were further averaged into 5 radial (C) and 4 vertical (D) groups. (E) Regions of center, middle, and edge were defined along the radial direction.

proline and sulfate grains was performed after combining 80 subsections into 20 averaged subsections; therefore, each averaged subsection of Fig. 2B was treated as $n = 1$. All the analyses were performed with a significance level of $P < 0.05$.

## RESULTS

*Stimulatory effect of tissue shear loading.* Proline and sulfate radiolabel incorporation into control disks was approximately 40 and 80 pmol/$\mu$g DNA/h, respectively, which is similar to values observed previously in newborn calf cartilage explants cultured under the same conditions (5). Radiolabel incorporation in dynamically sheared disks normalized to that of control disks is shown in Fig. 3A. Shear loading at 3% amplitude caused significant stimulation of protein by ~50% and proteoglycan by ~25% over static control ($P < 0.01$) at all frequencies tested (0.01, 0.1, and 1.0 Hz) (Fig. 3A). One-way ANOVA test showed that there was no trend of stimulation versus frequency in this range. The stimulatory effect at 1% strain amplitude was 41 and 25% for protein and proteoglycan synthesis, respectively, and was not significantly different from the stimulation at 3% strain at 0.1 Hz (Fig. 3A).

During loading, both the applied shear strain and the resulting shear stress waveforms were recorded. The applied shear strain waveform was essentially distortion-free; i.e., the THD was ≤0.5%. At 3% strain amplitude, the shear stress waveform sometimes showed THD in the range 3–15% (Fig. 1B). The higher value of THD (e.g., Fig. 1B, 0.01 Hz) indicates a small amount of slipping between cartilage disks and the chamber platens.

The shear loading configuration of Fig. 1A is called "simple shear" and is different from the "pure shear" configuration which can be applied by torsional loading of individual cylindrical disk specimens. Simple shear loading can induce low levels of fluid flow due to bending-induced pressure gradients localized near the leading and trailing peripheral edges of the explant disks (19). To check whether this fluid flow caused a local

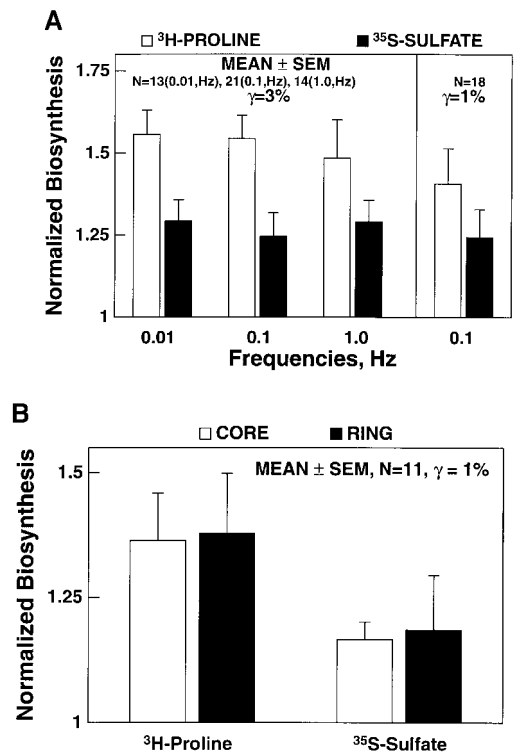


**FIG. 3.** Radiolabel incorporation (pmol/$\mu$g DNA/h) in dynamically sheared disks was normalized to that in control disks (control = 1). Syntheses of total protein and proteoglycan were significantly stimulated ~50 and ~25% over static control, respectively ($P < 0.01$), at 3% shear strain amplitude and frequencies of 0.01, 0.1, and 1.0 Hz. At 1% shear strain with a frequency of 0.1 Hz, protein and proteoglycan syntheses were stimulated by 41 and 25%, respectively, over control. However, there was no trend versus frequency in the biosynthesis at 3% shear strain (ANOVA, $P > 0.25$). The stimulatory effect was not significantly different between 1 and 3%. (B) In a separate series of experiments, shear strain of 1% at 0.1 Hz was applied to cartilage specimens. After loading, a 2-mm-diameter core was removed from the center region of each disk, leaving an outer annular ring of disks. Radiolabel incorporation was separately measured for the 2-mm core and outer annular ring. The stimulation of protein and proteoglycan in core and ring regions was not significantly different ($t$ test and power analysis, $P > 0.28$, *power* > 0.95).

stimulation of biosynthesis near the outer edges of the explants, we first compared the radiolabel incorporation in the 2-mm core regions with that of the annular ring after the application of 1% shear deformation for 24 h. Radiolabel incorporation (pmol/$\mu$g DNA/h) in the core and ring region of dynamically sheared disks was normalized to the core and ring regions of matched statically held control disks. In these experiments, shear deformation stimulated protein by 38% and proteoglycan by 18% over static controls in both the core and the ring region. Importantly, there was no significant difference between the normalized proline and sulfate incorporation rates in the cores and the outer annular rings of dynamically sheared disks ($P > 0.28$, *power* $> 0.95$) (Fig. 3B).

*Spatial analysis of newly synthesized protein and proteoglycan by autoradiography.* The spatial profiles of radiolabel incorporation were further analyzed by quantitative autoradiography. Proline and sulfate grain densities were quantified on one section from each of 24 disks from four groups tested. The relative increase in the grain densities of radiolabeled proline and sulfate of dynamically sheared disks was in good agreement with the relative increase by scintillation counting of total radiolabel incorporation measured on the other halves of the same disks ($\sim$50% for proline and $\sim$20% for sulfate). Images of chondrocytes and newly deposited matrices from center, middle, and edge regions of cartilage explants (Fig. 4) were used to analyze the radial and vertical variations of grain densities for proline and sulfate labeled sections (Figs. 5 and 6). Grain densities of dynamically sheared disks were normalized to the corresponding grain densities of control disks (second column (B and D) of Figs. 5 and 6). Overall, proline grain density was increased by 50%, and this stimulation was uniform along radial and vertical variations (Figs. 5B and 5D) as tested by one-way ANOVA ($P > 0.25$). In contrast, there was a significant trend in the radial variation of sulfate grains for both the shear and static control groups (by one-way ANOVA test, $P < 0.05$). Importantly, however, the normalized sulfate grain densities in dynamically sheared disks were highest in the center of the disk, not at the edge (Fig. 6C). Sulfate grain density did not vary significantly along the vertical direction (Fig. 6C and 6D).

## DISCUSSION

In the present study, dynamic tissue shear deformation of cartilage explants stimulated the synthesis of protein and proteoglycan significantly above levels in control explants held at the same offset static compression. The increase in synthesis did not depend strongly on frequency or strain within the frequency range 0.01–1.0 Hz and the 1–3% strain range tested. (We note, however, that in preliminary studies on disks cultured and tested in serum-free DMEM rather than 10% FBS, stimulation was not observed below 2% strain amplitude (data not shown).) The range of shear strains used in our study was motivated by previous experimental (24) and theoretical (18) studies of cartilage deformation relevant to joint loading *in vivo,* which predict that compressive and shear deformations of $\sim$1–3% may occur during dynamic or short-term loading. The shear loading used in this study was simple shear, which is different from a pure shear configuration. Pure shear loading does not cause any volumetric deformation or intratissue pressure gradient. Therefore, for homogeneous isotropic poroelastic materials, pure shear would not cause any intratissue fluid flow with respect to the solid matrix. However, simple shear deformation can enhance normal stresses at the leading and trailing edges of the disk in contact with the platens, which can induce local pressure gradients and relative fluid flow at these thin peripheral edge regions. Nevertheless, we chose the simple shear configuration (1) to apply a uniform shear deformation throughout the entire disk, since torsional deformation causes the strain to vary along the disk radial direction, and (2) to enable a simple approach to the use of multiple samples in each experiment for statistical analyses (Fig. 1A).

The effect of dynamic *shear* deformation in this study can be compared to that of dynamic *compressive* deformation over comparable ranges of frequency and strain. Dynamic compression between 0.01 and 1.0 Hz at 1–5% strain amplitude has been reported to stimulate the synthesis of proteins and proteoglycans (5, 13, 14, 22). Interestingly, dynamic *shear* deformation caused a twofold greater stimulation of protein synthesis than of proteoglycan synthesis, while dynamic *compression* appears to stimulate protein and proteoglycan synthesis by similar amounts. The previous finding that $\sim$80% of the [$^3$H]proline is incorporated into collagen in our newborn calf cartilage specimens (25) suggests that shear deformation may cause marked stimulation of collagen synthesis in our system. Quantitative autoradiographic analysis of newly synthesized proteoglycans within explant disks subjected to dynamic compression revealed an increase in proteoglycan synthesis with increasing disk radius compared to controls (13, 14). This radial variation in proteoglycan synthesis was similar to the radial variation in tissue-level fluid velocity predicted theoretically (14). In contrast, autoradiographic images of specimens subjected to shear deformation showed that [$^3$H]proline incorporation relative to controls was uniform throughout the disks (Fig. 5). The stimulation of [$^{35}$S]sulfate incorporation caused by shear (i.e., the normalized sulfate incorporation of Fig. 6B) decreased slightly with increasing radius. Taken together, these results suggest

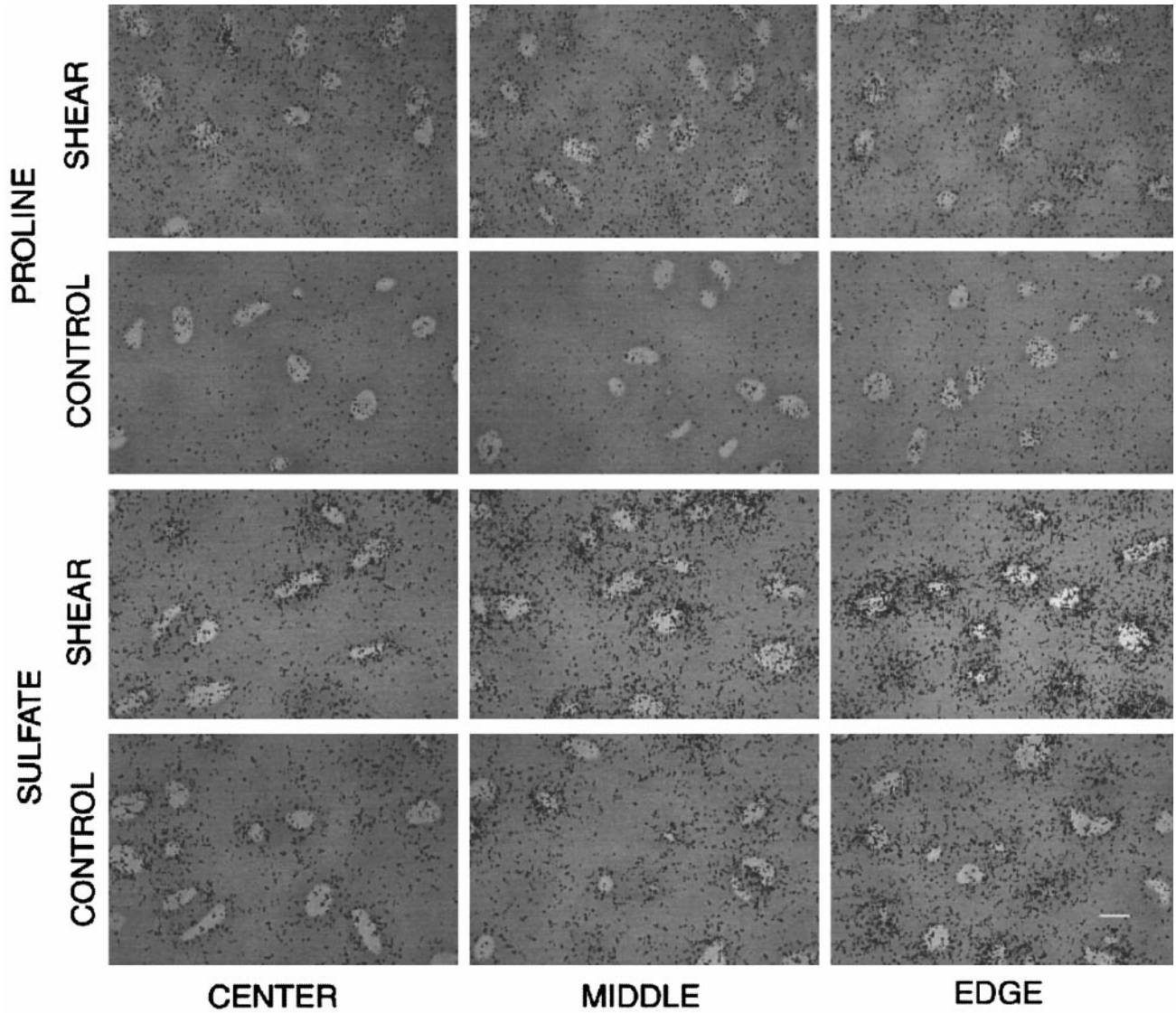


**FIG. 4.** Autoradiographic appearance of chondrocytes and proline and sulfate grains from center, middle, and edge regions of cartilage explants. Proline and sulfate grain density appeared higher in dynamically sheared disks than in static controls (white bar at the bottom right = 10 $\mu$m).

that the stimulatory effect of shear is not associated with tissue-level fluid flow which might have occurred at the edge regions. This conclusion is consistent with the fact that radial fluid flow in our simple shear configuration is estimated to be much smaller than in compression (see below). This hypothesis is also consistent with the core vs ring radiolabel incorporation data (Fig. 3B), which showed no macroscopic radial variation in synthesis in response to tissue shear.

In order to further delineate the physical stimuli associated with cell response to tissue shear deformation, a poroelastic model of the simple shear configuration of Fig. 1 for a 1% shear strain amplitude at 0.1 Hz was used (19, 26). Model predictions showed that the maximal fluid velocity over the 3-mm-diameter cross section was less than 0.02 $\mu$m/s, except at the 150-$\mu$m-wide outer edge at the platen–disk interface. Since the stimulation of proteoglycan synthesis by dynamic compression was estimated to occur in regions of the explant in which the fluid velocity was greater than 0.25 $\mu$m/s (14), we conclude that the much smaller and highly localized fluid flow in our simple shear configuration has minimal effect on biosynthesis. Of course, we cannot discount the possibility that cell-level (microscopic) changes in fluid flow patterns can be induced locally due to inhomogeneities in the material properties of extracellular matrix. The middle-zone newborn calf cartilage specimens used in this study do not exhibit the marked depth-dependent inhomogeneities of adult articular cartilage; rather, our immature carti-

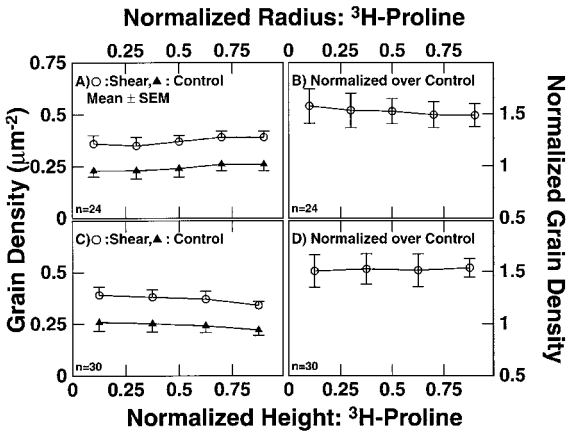


**FIG. 5.** (A) Proline grain density for shear and static control explants along radial direction. (B) Radial variation of grain densities of dynamically sheared explants normalized to controls (control = 1). (C) Proline grain density for shear and static control explants along vertical direction. (D) Vertical variation of grain densities of dynamically sheared explants normalized to controls (control = 1). Proline grains were uniformly distributed along radial and vertical directions, for both control and shear explants. Shear deformation caused uniform increase of grain densities along radial and vertical directions.

lage exhibits uniform matrix ultrastructure (5, 27). Therefore, inhomogeneities in the material properties of the pericellular versus interterritorial matrix (28) would more likely be the cause of any localized fluid flow patterns at the cell level. Such microscopic fluid motion due to cell-level inhomogeneities would occur over short distances and, therefore, decay faster in time than the tissue-level fluid flow that would result from volumetric compressive deformation. To address these issues, cell-level autoradiography methods (15) are now being used to quantify micrometer length–scale changes in radiolabel incorporation around individual chondrocytes through the cross section of these same specimens.

The effects of tissue shear can be compared to the known effects of fluid shear applied directly to cells. Fluid shear has been widely studied as a regulator of endothelial (29) and smooth muscle cells (30) as well as chondrocytes (28, 31). Fluid-induced shear stress applied to chondrocytes in monolayer culture has been found to alter cell morphology and matrix synthesis, to affect the production of PGE2, IL-6, TIMP-1, and nitric oxide (31), and to activate the ERK1/2 signaling pathway (32). However, chondrocytes in native tissue will experience much lower fluid velocities than the values used in these monolayer culture experiments (32). In addition, the shear stress applied to chondrocytes in fluid shear-monolayer culture studies is ~1 Pa, which must be distinguished from the more physiological 10–25 kPa shear stress caused by *tissue* shear deformation (18) in our study (Fig. 1). Under tissue shear deformation, most of the shear stress will be supported by the extracellular matrix due to the difference in shear stiffness between the ECM and cells, and chondrocytes will be deformed according to the surrounding matrix deformation. Therefore, the stimulatory effect of tissue shear deformation should most likely be considered a function of strain and not stress.

Taken together, our data suggest that the stimulation of biosynthesis by tissue shear is associated with events linked to deformation of extracellular matrix, cells, and intracellular matrix. This may also include changes in the facilitated transport of soluble factors through simultaneous matrix stretch and compaction. Such mechanical deformation may activate transduction pathways associated with the integrin–cytoskeleton machinery or stretch-activated channels (11). In addition to such upstream signaling pathways, mechanotransduction mechanisms in tissue shear may involve pathways further downstream related to changes in cell morphology. For example, shear deformation could affect protein translation and posttranslation modifications caused by changes in morphology of intracellular organelles. This hypothesis is supported by the recent EM studies (1) which showed changes in the ultrastructure of the rough endoplasmic reticulum, Golgi apparatus, and mitochondria of cartilage explants under graded levels of static compression. Future studies to identify the effect of shear deformation on mechanotransduction pathways at the upstream signaling, transcriptional, and posttranslational levels

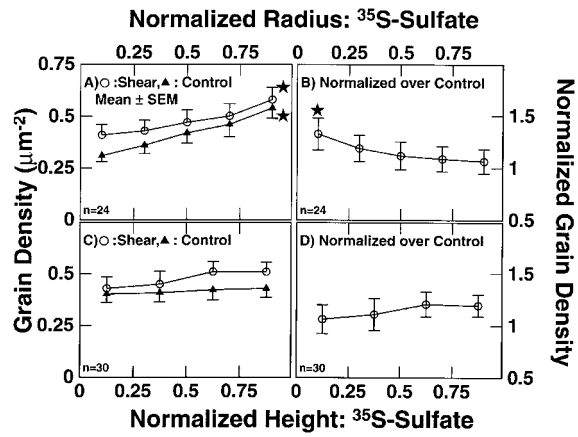


**FIG. 6.** Sulfate grain density for shear and static control explants along radial direction. (B) Radial variation of grain densities of dynamically sheared explants normalized to controls (control = 1). (C) Sulfate grain density for shear and static control explants along vertical direction. (D) Vertical variation of grain densities of dynamically sheared explants normalized to controls (control = 1). Sulfate grains showed radial variation (one-way ANOVA; $P < 0.01$) for control and shear groups (A). Normalized grain density showed a significant trend along radial direction (B) with higher stimulation at the center region. However, there were no trends along vertical directions for both groups and normalized sulfate grains (C and D).

should enhance our understanding of the mechanisms by which chondrocytes respond to mechanical deformation and concomitant physicochemical changes *in vivo*.

## ACKNOWLEDGMENTS

This research was supported by NIH Grant AR33236. We thank Elke Berger, Veronique Gaschen, and Prasanna Perumbuli for technical contributions.

## REFERENCES

1. Grodzinsky, A. J., Levenston, M. L., Jin, M., and Frank, E. H. (2000) *Annu. Rev. Biomed. Eng.* **2,** 691–713.
2. Hering, T. M. (1999) *Front. Biosci.* **4,** 743–761.
3. Smith, R. L., Trindade, M. C. D., Ikenoue, T., Mohtai, M., Das, P., Carter, D. R., Goodman, S. B., and Schurman, D. J. (2000) *Biorheology* **37,** 95–107.
4. Gray, M. L., Pizzanelli, A. M., Grodzinsky, A. J., and Lee, R. C. (1988) *J. Orthop. Res.* **6,** 777–792.
5. Sah, R. L., Kim, Y.-J., Doong, J. H., Grodzinsky, A. J., Plaas, A. H. K., and Sandy, J. D. (1989) *J. Orthop. Res.* **7,** 619–636.
6. Urban, J. P. G., Hall, A. C., and Gehl, K. A. (1993) *J. Cell. Physiol.* **154,** 262–270.
7. Parkkinen, J. J., Ikonen, J., Lammi, M. J., Laakkonen, J., and Tammi, M., and Helminen, H. J. (1993) *Arch. Biochem. Biophys.* **300,** 458–465.
8. Giori, N. J., Beaupre, G. S., and Carter, D. R. (1993) *J. Orthop. Res.* **11,** 581–591.
9. Sah, R. L. Y., Trippel, S. B., and Grodzinsky, A. J. (1996) *J. Orthop. Res.* **14,** 44–52.
10. Bonassar, L. J., Grodzinsky, A. J., Srinivasan, A., Davila, S. G., and Trippel, S. B. (2000) *Arch. Biochem. Biophys.* **379,** 57–63.
11. Wright, M., Jobanputra, P., Bavington, C., Salter, D. M., and Nuki, G. (1996) *Clin. Sci. Colch.* **90,** 61–71.
12. Millward-Sadler, S. J., Wright, M. O., Davies L. W., Nuki, G. and Salter, D. M. (2000) *Arthritis Rheum.* **43,** 2091–2099.
13. Kim, Y. J., Sah, R. L. Y., Grodzinsky, A. J., Plaas, A. H. K., and Sandy, J. D. (1994) *Arch. Biochem. Biophys.* **311,** 1–12.
14. Buschmann, M. D., Kim, Y. J., Wong, M., Frank, E. H., Hunziker E. B., and Grodzinsky, A. J. (1999) *Arch. Biochem. Biophys.* **366,** 1–7.
15. Quinn, T. M., Grodzinsky, A. J., Buschmann, M. D., Kim, Y. J., and Hunziker, E. B. (1998) *J. Cell Sci.* **111,** 573–583.
16. Wong, M., Siegrist, M., and Cao, X. (1999) *Matrix Biol.* **18,** 391–399.
17. Wilkins, R. J., Browning, J. A., and Urban, J. P. G. (2000) *Biorheology* **37,** 67–74.
18. Hou, J. S., Mow, V. C, Lai, W. M, and Holmes, M. H. (1992) *J. Biomech.* **3,** 247–259.
19. Frank, E. H., Jin, M., Loening, A., Levenston, M. L., and Grodzinsky, A. J. (2000) *J. Biomech.* **33,** 1523–1527.
20. Kim, Y. J., Sah, R. L. Y., Doong, J. Y. H., and Grodzinsky, A. J. (1988) *Anal. Biochem.* **174,** 168–176.
21. Buschmann, M. D., Maurer, A. M., Berger, E., and Hunziker, E. B. (1996) *J. Histochem. Cytochem.* **44,** 423–431.
22. Parkkinen, J. J., Lammi, M. J., Helminen, H. J., and Tammi, M. (1992) *J. Orthop. Res.* **10,** 610–620.
23. Lieber, R. L. (1990) *J. Orthop. Res.* **8,** 304–309.
24. Herberhold, C., Faber, S., Stammberger, T., Steinlechner, M., Putz, R., Englmeier, K. H., Reiser, M., and Eckstein, F. (1999) *J. Biomech.* **32,** 1287–1295.
25. Sah, R. L., Doong, J. Y., Grodzinsky, A. J., Plaas, A. H., and Sandy, J. D. (1991) *Arch. Biochem. Biophys.* **286,** 20–29.
26. Levenston, M. E., Frank, E. H., and Grodzinsky, A. J. (1998) *Comput. Methods Appl. Mech. Eng.* **156,** 231–246.
27. Hunziker, E. B. (1992) *in* Biological Regulation of the Chondrocytes, pp. 1–31, CRC Press, Boca Raton, FL.
28. Guilak, F., and Mow, V. C. (2000) *J. Biomech.* **33,** 1663–1673.
29. Jalali, S., del Pozo, M. A., Chen, K. D., Miao, H., Li, Y. S., Schwartz, M. A., Shyy, J. Y. J., and Chien, S. (2001) *Proc. Natl. Acad. Sci. USA* **98,** 1042–1046.
30. Rhoads, D. N., Eskin, S. G., and McIntire, L. V. (2000) *Arterioscler. Thromb. Vasc. Biol.* **20,** 416–421.
31. Smith, R. L., Donlon, B. S., Gupta, M. K., Mohtai, M, Das, P., Carter, D. R., Cooke, J., Gibbons, G., Hutchinson, N., and Schurman, D. J. (1995) *J. Orthop. Res.* **13,** 824–831.
32. Hung, C. T., Henshaw, R., Wang, C. C. B., Mauck, R. L., Raia, F., Palmer, G., Chao, P. H. G., Mow, V. C., Ratcliffe, A., and Valhmu, W. B. (2000) *J. Biomech.* **33,** 73–80.